# Dephasing model for spatially extended atomic states in cyclotronlike resonances

R. E. Wagner, S. Radovich, J. Gillespie, Q. Su, and R. Grobe
*Intense Laser Physics Theory Unit and Department of Physics, Illinois State University, Normal, Illinois 61790-4560*
(Received 13 June 2002; published 15 October 2002)

In recent work, the formation of ring-shaped electron distributions for hydrogen atoms in resonant static magnetic-laser fields has exclusively been associated with the impact of relativity. In this note we will generalize this statement and show that the nonlinearity associated with the nuclear binding force can trigger similarly shaped steady-state charge clouds in atoms under suitable conditions. The dephasing model, based on modeling the quantum-mechanical state by a classical ensemble of quasiparticles evolving with slightly different cyclotron periods, can recover features in the two lowest-order resonances as well as the Coulomb-field-induced charge distributions.

DOI: 10.1103/PhysRevA.66.043412 PACS number(s): 32.80.Rm

## I. INTRODUCTION

Even though the effect of static magnetic fields on the spectral properties of atomic and molecular energy eigenstates has been investigated widely in atomic physics [1], only recently has the interest shifted to the time-dependent response of atoms to a magnetic field. Several authors have investigated the impact of static magnetic fields on the scattered (higher-harmonic) light spectrum generated in strong field ionization [2–6] for various geometries with respect to the field directions. If the laser's polarization direction is aligned perpendicular to the direction of the static magnetic field, the electron can be resonantly excited into a relativistic orbit if the cyclotron frequency associated with the magnetic field, $\Omega \equiv eB/mc$, is commensurate with the laser frequency $\omega_L$. This resonance manifests itself spatially in a ring-shaped electronic charge cloud distribution which rotates around the nucleus. These charge distributions are reminiscent of mini-cyclotrons taking the size of an atom [7–9].

Usually the main optical method by which an atomic electron can acquire a relativistic speed involves an extremely powerful laser pulse [10,11], where the large force associated with the electric-field component of the laser is primarily responsible for accelerating the electron during a single cycle of the field. Atomic resonances, however, have not been exploited directly to bring an electron's speed up to the relativistic regime because an unlimited increase in the electron's speed at resonance is typically avoided by the nonlinearity of the atomic potential encountered by the large-amplitude motion. However, by exploiting the cyclotron-type resonance, an atom in a combined laser and magnetic field can be excited to a relativistic orbit without the need for an extremely powerful laser.

In the original work [7], the formation of the charge distributions was very crudely mimicked by a dephasing mechanism. Because of the inherent nonlinearity due to relativity in the system, one cannot find simple analytical formulas; in fact, for extreme velocities the system has been shown to be chaotic [12,13]. However, despite some progress, several important questions have remained unanswered. The most important one concerns the effect of the attractive force due to the atomic nucleus, which has not been investigated so far. Has the attractive Coulombic force a stabilizing or destabilizing effect on the ring-shaped electron charge clouds? Can the electronic ground state develop at all into the ring-shaped charge cloud if a strong atomic binding potential is present? In the more complicated case in which the cyclotron and laser frequencies are commensurate, more complicated charge cloud configurations, such as a rotating figure eight or propeller-shaped structures have been predicted [14,15]. Are these configurations at all permitted under a strong Coulombic binding situation? A second question concerns the validity of the dephasing approximation for modeling the nonlinearity for more general situations such as multiple or fractional resonances that are also associated with characteristic steady-state electronic distributions. A third and equally important class of questions needs to be addressed for a multielectron atom or ion. Can these charge distributions form at all when several electrons interact with each other? Can the electrons mutually exchange the energy resonantly absorbed from the laser? Can one expect differently shaped steady-state multielectron charge distributions?

Due to the enormous requirements on CPU time and memory for three-dimensional calculations, fully relativistic quantum simulations for these ring-shaped electron distributions have been performed only in two spatial dimensions [9]. In addition, computational limitations for the quantum simulations also required extremely large laser and cyclotron frequencies and very short interaction durations. At the present stage of computational development, only simulations that are based on classical but relativistic mechanics permit exploration in which (1) the laser and magnetic-field parameters are reasonable, (2) the problem is investigated in its full dimensionality, and (3) the electron-electron repulsion is taken fully into account.

The surprising validity of classical relativistic mechanics has been pointed out for various systems in which the predictions based on relativistic classical ensembles could be compared directly with exact numerical solutions to the time-dependent Dirac equation [16]. These comparisons were performed for free electrons in static electric fields, time-dependent electromagnetic fields in simple oscillator models [17], or bound electrons in rotating charge cloud distributions in two dimensions [9].

 

## II. THE IMPACT OF THE NUCLEUS ON CYCLOTRONIC CHARGE CLOUDS

In order to investigate the impact of the Coulomb force on the charge cloud, let us first briefly review the simple dephasing model proposed [7] to crudely mimic the formation of cyclotronic charge clouds due to the action of relativity. An electron in a static magnetic field of cyclotron frequency $\Omega$ and a time-dependent laser field of frequency $\omega_L$ is described (in atomic units) by

$$H=\{c^4+c^2[\mathbf{p}+(1/c)\mathbf{A}(\mathbf{r},t)]^2\}^{1/2} \tag{2.1}$$

where the vector potential $\mathbf{A}(\mathbf{r},t)$ is the sum of two parts, one modeling the laser field linearly polarized along the $x$ direction with field amplitude $E_0$, and the other corresponding to the static homogeneous magnetic field of strength $B_0$ along the $z$ direction:

$$\mathbf{A}(\mathbf{r},t)=\frac{c}{\omega_L}E_0\sin(\omega_L t-ky)\mathbf{e}_x+\frac{1}{2}\mathbf{r}\times(B_0\mathbf{e}_z). \tag{2.2}$$

The spiral-type (nonclosed) orbit of a single classical nonrelativistic electron can be crudely approximated in the $(x,y)$ plane by

$$x(t)=x_0+v_{x0}\sin(\Omega t)/\Omega+v_{y0}[\cos(\Omega t)-1]/\Omega -A[\cos(\Omega t)-\cos(\omega_L t)], \tag{2.3a}$$

$$y(t)=y_0+v_{y0}\sin(\Omega t)/\Omega-v_{x0}[\cos(\Omega t)-1]/\Omega -A[\sin(\Omega t)-\Omega\sin(\omega_L t)/\omega_L] \tag{2.3b}$$

with the amplitude $A\equiv E_0/(\omega_L^2-\Omega^2)$. Under near-resonant conditions ($\omega_L\approx\Omega$), the amplitude $A$ is so large that the initial conditions are irrelevant and the orbit $\mathbf{r}(t)=[x,y]$ is basically given by the sum of two rotating vectors, $\mathbf{r}(t)/A=\mathbf{r}_{\omega_L}(t)+\mathbf{r}_\Omega(t)$, where $\mathbf{r}_{\omega_L}(t)\equiv[\cos(\omega_L t),\Omega\sin(\omega_L t)/\omega_L]$ and $\mathbf{r}_\Omega(t)\equiv-[\cos(\Omega t),\sin(\Omega t)]$. For $\omega_L\approx\Omega$ the resulting motion is a spiral that quasiperiodically changes from inward to outward motion. If this simple model is applied to an ensemble of particles that differ by their initial conditions, $\mathbf{r}_0$ and $\mathbf{v}_0$, the distribution remains spatially localized. The natural spreading due to the initial dispersion in velocities is suppressed due to the confining static magnetic field that can lead to a quasiperiodic ''breathing'' motion [18]. The linearity of the nonrelativistic solution (2.3) with respect to the initial values $\mathbf{r}_0$ and $\mathbf{v}_0$ does not permit the nonrelativistic spatial density to spread beyond a maximum value given by the greater of $2\Delta v_{0x}/\Omega$ and $\Delta x_0$ and one would not expect solution (2.3) to predict the relativistic ring structures.

How does relativity affect the ensemble dynamics? As a very crude modification we can conjecture that the cyclotron frequency $\Omega$, which is independent of the velocity in the nonrelativistic case, depends on the speed. This conjecture is supported by the relativistic electron motion in a magnetic field in the absence of the time-dependent electric field for which the cyclotron frequency takes the velocity-dependent form $\Omega_{\rm rel}=\Omega\sqrt{[1-(v/c)^2]}$ [19]. To reflect different initial velocities in the ensemble, we permit the parameter $\Omega$ to fluctuate slightly from trajectory to trajectory: $\Omega\rightarrow\Omega\text{-}\Delta\Omega$. The small dephasing $\Delta\Omega$, used to mimic the velocity-dependent relativistic cyclotron frequencies, was chosen to depend on the initial velocity, $\Delta\Omega=\Delta\Omega(\mathbf{v}_0)$. When the interaction time exceeds $2\pi/\langle\Delta\Omega\rangle$, where $\langle\Delta\Omega\rangle$ is the average size of the fluctuation, the phase $(\Omega\text{-}\Delta\Omega)t$ in $\mathbf{r}_\Omega(t)$ is fully randomized, and the ensemble particles fill up the circumference of the $\Omega$ circle. The oscillating terms with the phase $\omega_L t$ in $\mathbf{r}_{\omega_L}(t)$, however, stay coherently in phase. As a result, the center of motion of the ring-shaped charge distribution is described by the quasicircular motion $\mathbf{r}_{\omega_L}(t)$. It is quite remarkable that such a simple dephasing mechanism based on strong velocity dispersion can model the relativistic dynamics even quantitatively if the free parameter $\Delta\Omega(\mathbf{v}_0)$ is chosen appropriately.

We should mention that the ring-shaped charge cloud actually covers the surface of a cylinder, as there is no force present which inhibits the free spreading of the particles along the $z$ direction. The characteristics of the evolution are summarized in Fig. 1 after interaction with the fields for 2000 laser cycles. For better comparison with the following discussion, the Coulomb potential was turned off in Fig. 1.

The trajectories were solved in canonical variables using a Runge-Kutta fourth-order algorithm with self-adapting step size. This algorithm is very accurate and reliable, which is necessary if very high-frequency components of the orbits need to be resolved.

Next we will generalize the dephasing model and show that the formation of a ring need not be exclusively associated with relativity but can also be triggered by the nonlinearity associated with the Coulombic binding potential of the nucleus. We have repeated the simulation for the same parameters as in Fig. 1, but this time we have turned relativity off [which can be easily achieved by replacing the parameter $c$ in Eq. (2.1) with infinity, except for the $1/c$ factor in front of $\mathbf{A}$]. In return we allowed for the nuclear interaction that is modeled by a screened Coulomb potential $V(r)=-1/\sqrt{[r^2+1]}$:

$$H=\frac{1}{2}\left(\mathbf{p}+\frac{1}{c}\mathbf{A}(\mathbf{r},t)\right)^2+V(r). \tag{2.4}$$

It has been demonstrated [20] that predictions of classical trajectories associated with this screened Coulomb potential approximate the quantum-mechanical calculations for the $-1/r$ potential much more closely than those obtained classically with the singular $-1/r$ potential binding.

In Fig. 2 we present a scattergram of the ensemble points after an interaction of $T=2000$ laser cycles. The formation of a ring similar to that in Fig. 1 is apparent. A comparison with the simulation in which relativity was included but $V(r)$ excluded suggests that the formation of the Coulomb-force-induced ring can occur on a faster time scale. In addition, the long-range attractive force associated with $V(r)$ reduces the spreading along the $z$ direction. In fact, the wedgelike shape displayed in the $(x,z)$ plane suggests that the closer the trajectories are to the nucleus at $\mathbf{r}=(0,0,0)$, the more the spreading along the $z$ direction is suppressed.

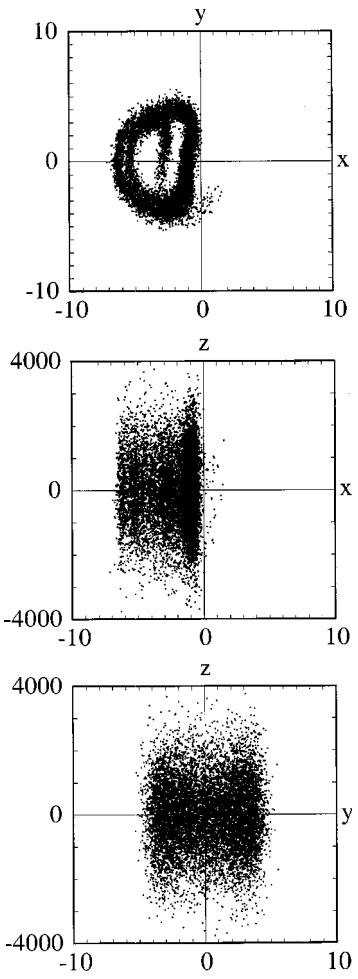


FIG. 1. Cyclotronic charge clouds induced by relativity. The spatial distribution of the electron charge cloud after the interaction with the combined laser-magnetic field. The Coulomb force field was turned off during the interaction. ($T=2000\times 2\pi/\omega_L$, $E_0=1$ a.u., $\omega_L=5$ a.u., $\Omega=5.02$ a.u., 10 000 quasiparticles with initial phase space uncertainties $\Delta x=1$ a.u., $\Delta p=0.5$ a.u., all axes in a.u.)

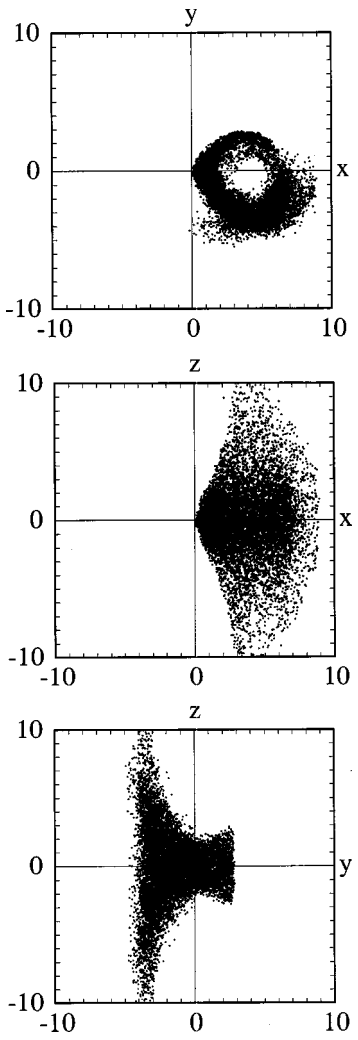


FIG. 2. Cyclotronic charge clouds induced by the nonlinear binding force. The spatial distribution of the electron charge cloud after the interaction with the combined laser-magnetic field. The effect of relativity was turned off during the interaction. ($T=2000\times 2\pi/\omega_L$, $E_0=1$ a.u., $\omega_L=5$ a.u., $\Omega=5.02$ a.u., 10 000 quasiparticles with initial uncertainties $\Delta x=1$ a.u., $\Delta p=0.5$ a.u., all axes in a.u.)

How can one model the Coulomb-force-induced ring structure? In contrast to the relativistic dephasing, which is based on a velocity-dependent cyclotron frequency, we can now assume that this frequency does depend on the initial position in the potential. In fact, to be more precise, there are no simple analytical solutions known for the special case of an electron in the binding potential and the static magnetic field. In contrast to the strictly periodic relativistic motion in the magnetic field without any binding potential, the nonrelativistic orbit in a binding force cannot even be described by a single frequency as the orbits are not closed. It turns out that a simple replacement of the cyclotron frequency with a position-dependent one qualitatively reproduces the formation of the ring.

### III. THE DEPHASING MODEL TO MIMIC RELATIVISTIC EFFECTS FOR FRACTIONAL RESONANCES

In Sec. II, the impact of nonlinearity associated with either relativity or the Coulombic force was modeled within the dephasing approximation characterized by a different effective cyclotron frequency for each ensemble particle. The precise value of this frequency was given by either the initial velocity (to mimic the action of relativity) or the initial position (to mimic the action of the Coulombic force). In the following we will show that this simple dephasing mechanism can even predict the charge distributions associated with the lowest fractional resonance. In previous work [7,14,15] we have shown that if the cyclotron frequency $\Omega$ is commensurate with the laser's frequency $\omega_L$, i.e., $\Omega/\omega_L \approx n/m$ with integer values of $n$ and $m$, rotating steady-state charge distributions of various shapes can be obtained.

We will focus here on the simplest fractional resonance, $\Omega/\omega_L \approx 1/2$. In Fig. 3 we display snapshots of the dynamics that show the formation of a rotating figure-eight-like charge density. The data were obtained by solving the full relativistic equation (2.1) for 10 000 quasiparticles with $E_0$

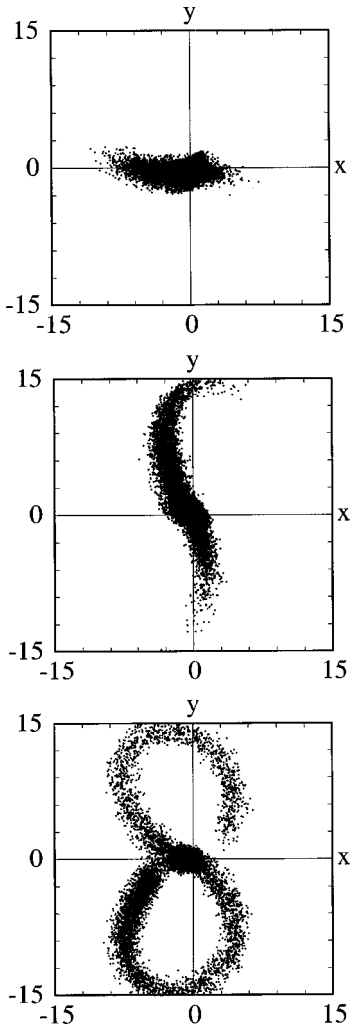


FIG. 3. Effect of relativity on cyclotronic charge clouds at a fractional resonance. The spatial distribution of the electron charge cloud after times $T=38$, 58, and 100 laser cycles. ($E_0=10$ a.u., $\omega_L=5$ a.u., $\Omega=2.51$ a.u., 10 000 quasiparticles with initial uncertainties $\Delta x=0.5$ a.u., $\Delta p=1$ a.u., all axes in a.u.)

$=10$ a.u., $\omega_L=5$ a.u., and $\Omega=2.51$ a.u.

There are various interaction mechanisms that can lead to the qualitative features of the time evolution: (1) the nonlinearity associated with relativity, (2) the magnetic-field component of the electromagnetic radiation field, (3) the electric-field component of the field, and (4) details of the initial state. In order to separate out irrelevant effects we have rewritten the laser part of the vector potential $\mathbf{A}(\mathbf{r},t)=(c/\omega_L)E_0\sin(\omega_L t\text{-}ky)\mathbf{e}_x$ in terms of the space- and time-dependent electric and magnetic fields $\mathbf{E}(y,t)=E_0\cos(\omega_L t\text{-}ky)\mathbf{e}_x$ and $\mathbf{B}(y,t)=E_0\cos(\omega_L t\text{-}ky)\mathbf{e}_z$, and solved the corresponding relativistic Newton equations.

In order to identify the main mechanism for the formation of the figure eight we have repeated our simulations for various limiting conditions. It turns out that in the absence of relativity the charge cloud develops from its initial spherically symmetric distribution into a rotating-stick shape. The main characteristics of this rotating stick are basically preserved even if the magnetic field component of the laser $B(y,t)$ is "mathematically" turned off. If we assume that the elongation along the $y$ direction is not too large, we can Taylor-expand the electric-field component of the laser field $E_0\sin(\omega_L t\text{-}ky)$ as $E_0\sin(\omega_L t)-E_0 ky\cos(\omega_L t)$. It turns out that the zeroth-order term $E_0\sin(\omega_L t)$ has only a minor influence on the rotating stick. In other words, the basic evolution to the figure-eight distribution is contained in the simple set of differential equations

$$\frac{d^2}{dt^2}x=E_0 ky\cos(\omega_L t)-(B_0/c)\sqrt{1-(v/c)^2}\,\frac{d}{dt}y, \tag{3.1a}$$

$$\frac{d^2}{dt^2}y=(B_0/c)\sqrt{1-(v/c)^2}\,\frac{d}{dt}x, \tag{3.1b}$$

$$\frac{d^2}{dt^2}z=0. \tag{3.1c}$$

Here we have approximated relativity with the gamma factor $\sqrt{1-(v/c)^2}$. This set of equations includes the absolute minimum number of ingredients to predict the figure eight. Unfortunately, despite the numerous approximations, these equations still cannot be solved analytically. The nonrelativistic case ($v/c=0$) can be solved if we put the factor $\cos(\omega_L t)$ in Eq. (3.1a) equal to 1. The right-hand side of the equation is not explicitly time dependent and predicts the formation of the stick:

$$x(t)=x_0+[A_1\lambda_1\exp(\lambda_1 t)+A_2\lambda_2\exp(\lambda_2 t)+A_3\lambda_3\exp(\lambda_3 t)-v_{y0}]c/B_0, \tag{3.2a}$$

$$y(t)=A_1\exp(\lambda_1 t)+A_2\exp(\lambda_2 t)+A_3\exp(\lambda_3 t), \tag{3.2b}$$

where the coefficients $A_i$ ($i=1,2,3$) are given by the initial conditions. The time scales are characterized by the three eigenvalues

$$\lambda_1=[-\sqrt[3]{62}(B_0/c)^2+\sqrt[3]{4}D]/(6D), \tag{3.2c}$$

$$\lambda_2=[\sqrt[3]{62}(B_0/c)^2-\sqrt[3]{4}D]/(D\sqrt[3]{248})+i[\sqrt[3]{62}(B_0/c)^2+\sqrt[3]{4}D]/(D\sqrt[3]{248}), \tag{3.2d}$$

$$\lambda_3=[\sqrt[3]{62}(B_0/c)^2-\sqrt[3]{4}D]/(D\sqrt[3]{248})-i[\sqrt[3]{62}(B_0/c)^2+\sqrt[3]{4}D]/(D\sqrt[3]{248}), \tag{3.2e}$$

where

$$D\equiv\sqrt[3]{27(B_0E_0k/c)+\sqrt{108(B_0/c)^6+729(B_0E_0k/c)^2}}.$$

The explicit forms for $A_i$ are

$$A_1=-\frac{-b_3\lambda_2+b_2\lambda_2^2-b_2\lambda_2\lambda_3+b_2\lambda_3^2-b_1\lambda_2^2\lambda_3^2}{(\lambda_1-\lambda_2)(\lambda_1-\lambda_3)(\lambda_1\lambda_2+\lambda_1\lambda_3+\lambda_2\lambda_3)}, \tag{3.2f}$$

$$A_2=-\frac{b_3\lambda_1-b_2\lambda_1^2+b_3\lambda_3-b_2\lambda_1\lambda_3-b_2\lambda_3^2+b_1\lambda_1^2\lambda_3^2}{(\lambda_1-\lambda_2)(\lambda_2-\lambda_3)(\lambda_1\lambda_2+\lambda_1\lambda_3+\lambda_2\lambda_3)}, \tag{3.2g}$$

$$A_3=-\frac{-b_3\lambda_1+b_2\lambda_1^2-b_3\lambda_2+b_2\lambda_1\lambda_2+b_2\lambda_2^2-b_1\lambda_1^2\lambda_2^2}{(\lambda_1-\lambda_3)(\lambda_2-\lambda_3)(\lambda_1\lambda_2+\lambda_1\lambda_3+\lambda_2\lambda_3)}, \tag{3.2h}$$

where $b_1\equiv y_0$, $b_2\equiv B_0v_{x0}/c$, $b_3\equiv E_0B_0ky_0/c-(B_0/c)^2v_{y0}$. The $y$-dependent force $E_0ky$ along the $x$ direction is mainly responsible for the formation of the stick. The solutions of Eqs. (3.2) have an easy long-time limit, $x=x_0+A_1\lambda_1c[\exp(\lambda_1t)-1]/B_0$ and $y=B_0x/(c\lambda_1)$. Due to the absence of the rotating factor $\cos(\omega_Lt)$, the stick does not rotate and its final angle with the $x$ axis is determined by the ratio $B_0/(c\lambda_1)$. We note that the initial velocities $v_{x0}$ and $v_{y0}$ are crucial in determining into which quadrant the respective particle evolves. Particles with initial positive velocities evolve in the first quadrant, whereas those with negative speed evolve into the third one. The absence of relativity as well as the factor $\cos(\omega_Lt)$ permits the particles to gain unbounded speeds as they evolve.

The time-dependent factor $\cos(\omega_Lt)$ seems to be crucial for the rotation of the stick, but unfortunately the equations of motion cannot be solved analytically. In order to test the main ideas of dephasing for this work, we need an analytical expression. The spiral-type nonrelativistic orbits suggest that one can very crudely mimic the time evolution of the rotating stick by the following expressions:

$$x(t)=x_0+R(t)\cos(\Omega t) \tag{3.3a}$$

$$y(t)=y_0+R(t)\sin(\Omega t), \tag{3.3b}$$

$$z(t)=z_0+V_{z0}t. \tag{3.3c}$$

The exact time-dependent radius of the stick $R(t)$ is probably a nontrivial function of time, but for reasons of simplicity we have approximated it here by the simple sinusoidal function of the initial velocities

$$R(t)=\alpha_1\sin[\alpha_2(v_{x0}+v_{y0})t]. \tag{3.3d}$$

The choice of the frequency factor $(v_{x0}+v_{y0})$ is crucial to reflect the correct dependence of the initial speed at either the upper or the lower part of the stick.

Now we are ready to test the dephasing model for a fractional resonance. For each particle, we replace the cyclotron frequency $\Omega$ by a modeled "Lorentz contracted" value $\Omega-\Delta\Omega$, where the dephasing term $\Delta\Omega=\alpha_2|v_{x0}+v_{y0}|$. Each particle has now a slightly different cyclotron period. Instead of climbing up and down the rotating stick, the particles get out of phase with respect to each other, leading to the figure eight. The distribution of the corresponding ensemble for the parameters $\alpha_1=15$ and $\alpha_2=1/160$ is shown in Fig. 4. The distribution qualitatively agrees with Fig. 3 and validates the simple dephasing model for fractional resonances.

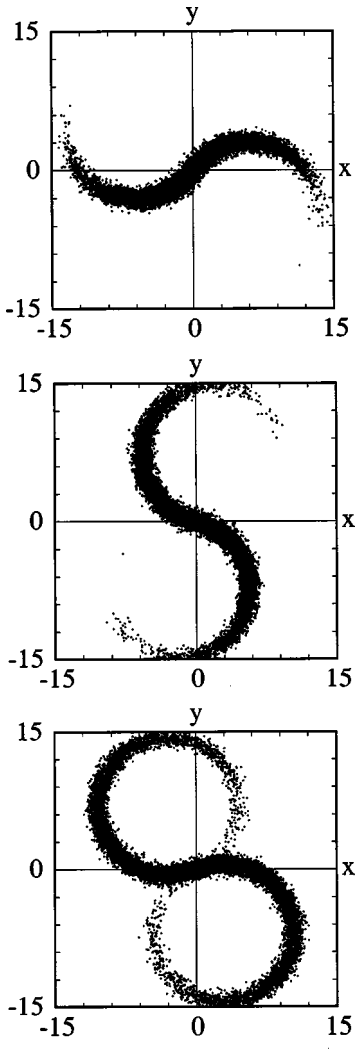


FIG. 4. The relativistic dephasing model for a fractional resonance. The spatial distribution of the electron charge cloud according to the dephasing model described in Eq. (3.3) with the parameters $\alpha_1=15$ and $\alpha_2=1/160$ at the same instants as in Fig. 3. ($\Omega=2.51$ a.u., 10 000 quasiparticles with initial uncertainties $\Delta x=0.5$ a.u., $\Delta v=1$ a.u., all axes in a.u.)

## IV. DISCUSSION

There are two main conclusions from the current work. First, in contrast to the previous belief, the formation of cyclotronic charge clouds does not necessarily require exclusively the effects of relativity. In fact, the nonlinearity associated with the Coulombic binding potential may also lead to the formation of a similar ring-shaped steady-state distribution of electrons in combined magnetic and laser fields. In contrast to relativistic dephasing, however, the presence of the nuclear binding force keeps the charge cloud from spreading along the magnetic-field lines. Independent of the cause of the nonlinearity, the formation of the charge distributions can be described by a simple dephasing model in the coordinate and momentum variables. In this model each particle representing the quantum wave function is assigned a slightly different cyclotron frequency that depends on either the initial velocity or position.

Second, for fractional resonances, cyclotronic charge clouds can take the form of a simple rotating figure-eight-shaped distribution. These are based in part on the nonlinearity associated with the position-dependent part of the laser field. Unfortunately, the simplest possible equation presenting the nonrelativistic behavior cannot be solved analytically. However, simple model expressions can be found that mimic the nonrelativistic behavior and the dephasing approximation qualitatively reproduces the relativistic behavior.

In summary, we should point out that we have not been able to find a universal approach that can explain the entire manifold of steady-state electron charge distribution characteristics for all multiple and fractional resonances. Even though in the three cases examined so far the dephasing scheme seems to work qualitatively, the generality of this approximation is not completely clear at the moment. One might point out that for many parameters which lead to resonancelike behavior the required degree of nonlinearity might even make the dynamics chaotic, even though the steady-state electron distributions appear to be relatively regular. As an example of the curious structures and also an outlook for future investigations, we display in Fig. 5 the final charge distributions for two different sets of field parameters. In the first case the ground state evolves into a rotating triangle, in the second case the steady-state distribution is a rotating four-bladed propeller. Clearly much more work needs to be done in this area to model and finally understand these charge configurations.

It is obvious that the present work will raise more questions than it can answer. The relativistic interaction of laser-driven electrons in extremely strong static homogeneous magnetic fields is a relatively unexplored area. The strengths of the $B$ fields discussed in this work are certainly smaller than those of neutron stars, but on the other hand they are several orders of magnitude larger than the static fields generated by nondestructive magnets in a laboratory setup in the millisecond range [21]. Recently, Kudasov *et al.* [22] have produced static magnetic field bursts of microsecond duration and a maximum amplitude of 1000 T.

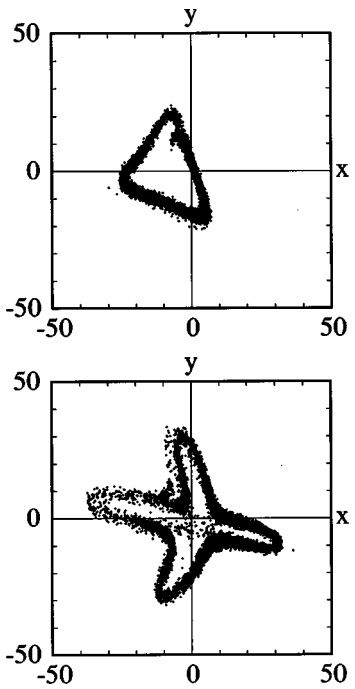


FIG. 5. Steady-state charge distributions. (Top) The ''triangular'' spatial electron charge distribution. ($E_0=150$ a.u., $\omega_L=5$ a.u., $\Omega=1.57$ a.u., 10 000 quasiparticles with initial uncertainties $\Delta x=0.5$ a.u., $\Delta v=1$ a.u., all axes in a.u.) (Bottom) The ''four-bladed propeller'' spatial electron charge distribution. ($E_0=150$ a.u., $\omega_L=5$ a.u., $\Omega=1.257$ a.u., 10 000 quasiparticles with initial uncertainties $\Delta x=0.5$ a.u., $\Delta v=1$ a.u., all axes in a.u.)

## ACKNOWLEDGMENT

This work has been supported by the NSF under Grant No. PHY-0139596. We also acknowledge support from the Research Corporation for Cottrell Science Awards and ISU for URGs. R.E.W. and J.G. thank the Illinois State University Undergraduate Honors Program for support of this research work.

[1] For reviews of hydrogen atoms in homogeneous magnetic fields, see H. Friedrich and D. Wintgen, Phys. Rep. **183**, 37 (1989); H. Hasegawa, M. Robnik, and G. Wunner, Prog. Theor. Phys. Suppl. **98**, 198 (1989); H. Ruder, G. Wunner, H. Herold, and F. Geyer, *Atoms in Strong Magnetic Fields* (Springer-Verlag 1994).

[2] T. Zuo, A. D. Bandrauk, M. Ivanov, and P. B. Corkum, Phys. Rev. A **51**, 3991 (1995).

[3] J. P. Connerade and C. H. Keitel, Phys. Rev. A **53**, 2748 (1996).

[4] Y. I. Salamin and F. H. M. Faisal, Phys. Rev. A **54**, 4383 (1996); **58**, 3221 (1998).

[5] R. E. Wagner, Q. Su, and R. Grobe, Phys. Rev. A **60**, 3233 (1999).

[6] D. B. Milosevic and A. F. Starace, Phys. Rev. Lett. **82**, 2653 (1999).

[7] R. E. Wagner, Q. Su, and R. Grobe, Phys. Rev. Lett. **84**, 3282 (2000).

[8] I. Peterson, Sci. News (Washington, D. C.) **157**, 287 (2000).

[9] P. Krekora, R. E. Wagner, Q. Su, and R. Grobe, Phys. Rev. A **63**, 25404 (2001).

[10] G. A. Mourou, C. P. J. Barty, and M. D. Perry, Phys. Today **51(1)**, 22 (1998); M. D. Perry and G. Mourou, Science **264**, 917 (1994).

[11] G. A. Mourou and D. Umstadter, Sci. Am. (May, 2002).

[12] J.-H. Kim and H.-W. Lee, Phys. Rev. E **51**, 1579 (1995).

[13] J.-H. Kim and H.-W. Lee, Phys. Rev. E **54**, 3461 (1996).

[14] P. J. Peverly, R. E. Wagner, Q. Su, and R. Grobe, Laser Phys. **10**, 303 (2000).

[15] Q. Su, R. E. Wagner, P. J. Peverly, and R. Grobe, in *Frontiers of Laser Physics and Quantum Optics*, edited by Z. Xu, S. Xie, S.-Y. Zhu, and M. O. Scully (Springer, Berlin, 2000), p. 117.

[16] J. W. Braun, Q. Su, and R. Grobe, Phys. Rev. A **59**, 604 (1999).
[17] R. E. Wagner, P. J. Peverly, Q. Su, and R. Grobe, Phys. Rev. A **61**, 35402 (2000).
[18] J. C. Csesznegi, G. H. Rutherford, Q. Su, and R. Grobe, Laser Phys. **9**, 41 (1999).
[19] For temporal quantum revivals due to relativistic velocities in homogeneous fields, see P. Filipowicz and J. Mostowski, Phys. Phys. Lett. **86A**, 356 (1981).
[20] M. Gajda, J. Grochmalicki, M. Lewenstein, and K. Rzazewski, Phys. Rev. A **46**, 1638 (1992).
[21] For a review on developments of nondestructive 100 T magnets, see Phys. Today **51(10)**, 21 (1998).
[22] Yu. B. Kudasov *et al.*, JETP Lett. **68**, 350 (1998).